Vietnam Journal of Mechanics, NCST of Vietnam Vol. 21, 1999, No 1 (8 – 24)

COMBINATION OF COLLOCATION AND FACTORIZATION METHODS APPLIED TO NUMERICAL SOLUTIONS OF BUBBLE-INSIDE DROP SYSTEM DYNAMICS

DUONG NGOC HAI
Institute of Mechanics, NCST of Vietnam

ABSTRACT. In the paper the combination of collocation and factorization methods applied to numerical investigation of bubble-inside drop system dynamics is presented. Initially assumed bubble and drop have ellipsoidal forms. The initial relative location of the drop in the bubble is determined by equilibrium condition between drop weight and lift-force due to pressure distribution in gas/vapor. Calculations are implemented for the case of spherical bubble, drop without and with vaporization (thermal effect) and for the experimental case [6] with alumini drop in water in pressure waves.

1. Introduction

The investigation of behavior of the system of drop and vapor cover (Fig. 1) is important for analysis of different possible kind of situation may be met in chemical, energetic industries and cryogen techniques. To describe dynamics of this system the mathematical model improving existed models taking into account thermal effect and vaporization at bubble wall is proposed in [3]. In this paper using combination of collocation and factorization methods some calculation results are presented.

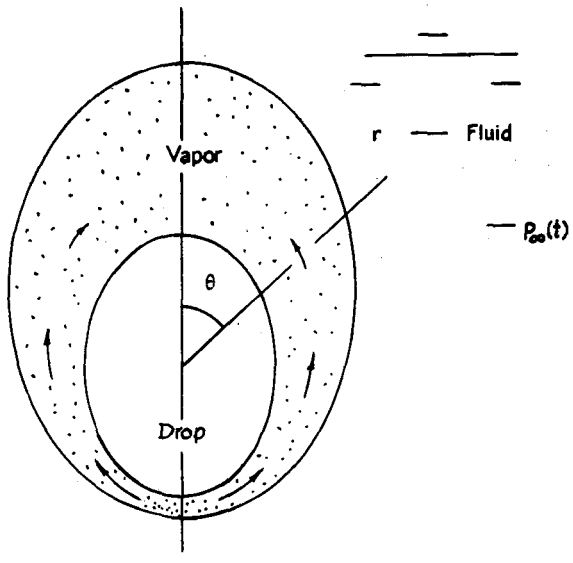

Fig. 1

2. Mathematical formulation

The model with rotational symmetry consists of following equations:

* for outside liquid flow:

$$\nabla^2\Phi = 0, \qquad \vec{u}_\ell = \nabla\Phi, \tag{2.1}$$

$$\frac{\partial\Phi}{\partial t} = -\frac{1}{2}\nabla\Phi\cdot\nabla\Phi - g\,\cos\theta - \frac{p_\nu - p_\infty(t)}{\rho_\ell} \tag{2.2}$$

$$-\frac{\sigma}{\rho_\ell R}\left\{\frac{1+2\left(\frac{1}{R}\frac{\partial R}{\partial\theta}\right)^2 - \frac{1}{R}\frac{\partial^2 R}{\partial\theta^2}}{\left[1+\left(\frac{1}{R}\frac{\partial R}{\partial\theta}\right)^2\right]^{3/2}} + \frac{1-\frac{1}{R}\frac{\partial R}{\partial\theta}\frac{\cos\theta}{\sin\theta}}{\left[1+\left(\frac{1}{R}\frac{\partial R}{\partial\theta}\right)^2\right]^{1/2}}\right\},$$

$$r\to\infty: \qquad \vec{u}_\ell \to 0, \tag{2.3}$$

$$t=0: \qquad \vec{u}_\ell = 0, \tag{2.4}$$

$$\left(\nabla^2 = \frac{1}{r^2}\frac{\partial}{\partial r}\left(r^2\frac{\partial}{\partial r}\right) + \frac{1}{r^2\sin\theta}\frac{\partial}{\partial\theta}\left(\sin\theta\frac{\partial}{\partial\theta}\right),\right.$$

$$\left.\Phi = \Phi(r,\theta,t), \qquad \frac{d\Phi}{dt}\Big|_\theta = \frac{\partial\Phi}{\partial t} + \frac{\partial\Phi}{\partial r}\frac{\partial r}{\partial t}\right).$$

where $\vec{u}$ is velocity vector; p and ρ are pressure and density, respectively; g is gravitational acceleration; σ is surface tension coefficient; R_b is bubble radius; r is radial coordinate; θ is polar distance, and t is time. The subscripts ℓ, g (or v) and ∞ refer to parameters of liquid, gas (vapor) and at infinity, respectively.

* for inside gas flow:

$$\frac{\partial}{\partial t}\left(\frac{R_b^3 - R_d^3}{3}\rho_\nu\right) + \frac{1}{\sin\theta}\frac{\partial}{\partial\theta}\left(\frac{R_b^2 - R_d^2}{2}\rho_\nu u_\nu\sin\theta\right) = j\dot{\overline{R}}^2, \tag{2.5}$$

$$u_\nu = -\frac{(R_b - R_d)^2}{k\mu_\nu(R_b + R_d)}\frac{\partial p_\nu}{\partial\theta}. \tag{2.6}$$

$$\begin{aligned} &p_\nu = p_{\nu 0}(\rho_\nu/\rho_{\nu 0})^n, && j = (q_\nu + q_\ell + q_r)/\ell_{eq},\\ &q_r = B\varepsilon(T_d^4 - T_s^4), && q_\ell = -\lambda_\ell(T_s - T_\infty)/\delta,\\ &q_\nu = \lambda_\nu(T_d - T_s)/(R_b - R_d), && \ell_{eq} = \ell + 0.68c_\nu(T_d - T_s), \end{aligned} \tag{2.7}$$

$$\frac{dT_s}{dp_\nu} = \frac{T_s}{\ell\rho_\nu}\left(1 - \frac{\rho_\nu}{\rho_\ell}\right).$$

$$\theta = 0, \quad \frac{\partial p_\nu}{\partial\theta} = 0, \qquad \theta = \pi, \quad \frac{\partial p_\nu}{\partial\theta} = 0. \tag{2.8}$$

$$t = 0, \quad p_\nu(0,\theta) = p_{\nu 0}(\theta), \qquad \rho_\nu = \rho_{\nu 0}(\theta), \quad u_\nu = u_{\nu 0}(\theta) \tag{2.9}$$

* for definition of moving boundary:

$$\frac{dR}{dt} = \left(\frac{\partial \Phi}{\partial r} + \frac{1}{R^2}\frac{\partial \Phi}{\partial \theta}\frac{\partial R}{\partial \theta}\right) \tag{2.10}$$

$$R(\theta, 0) = R_0(\theta). \tag{2.11}$$

The system of eqs. (2.1)-(2.11) is closed and can be used to describe behavior of the system of drop and vapor cover. More details about the mathematical description can be seen in [3].

3. Dimensionless parameters

By standard procedure the system of proposed equations can be transformed into the dimensionless form. It could be shown that the solution of above system of equations depends on the following dimensionless parameters which, respectively, characterize:

the geometrical properties of, e.g. rotational symmetry ellipsoid drop and bubble:

$$\overline{R}_{dh} = R_{dh}/R_0, \quad \overline{R}_{b\nu 0} = R_{b\nu 0}/R_0, \quad \overline{R}_{bh} = R_{bh}/R_{b\nu},$$

the thermophysical properties of the materials:

$$n, \quad Re_\nu = \frac{\rho_0 a_0 R_0}{\mu_\nu}, \quad k, \quad \overline{\sigma} = \frac{\sigma}{p_0 R_0}, \quad \overline{\rho}_\ell = \frac{\rho_\ell}{\rho_0}, \quad \overline{\rho}_d = \frac{\rho_d}{\rho_0}$$

the heat and mass transfer process:

$$\overline{c}_\nu = c_\nu T_0/\ell, \quad \overline{\lambda}_\ell = \lambda_\ell/\lambda_0, \quad \overline{\delta} = \delta/R_0, \quad \overline{\varepsilon} = B\varepsilon T_0^4/\lambda_0 R_0,$$
$$\overline{T}_d = T_d/T_0, \quad J_0 = \lambda_0 T_0/R_0 \ell a_0 \rho_0,$$

the gravity: $\overline{g} = gR_0/p_0$

and the pressure disturbances:

$$\overline{p}_\infty = p_\infty/p_0 \quad \text{or} \quad \Delta\overline{p}_\infty = (P_\infty - p_0)/p_0.$$

Here $R_0 = R_{d\nu}$, $\rho_0 = \rho_{\nu 0}$, $\lambda_0 = \lambda_\nu$, $a_0^2 = np_0/\rho_0$. Together 17 dimensionless parameters characterize the considered problem!

4. Initial installation: vapor density, pressure and velocity distribution

The initial state of the system is determined by requiring force balance between the lift-force due to pressure distribution in vapor and drop weight. Initially assumed drop and bubble have ellipsoidal forms.

a) The weight of drop:

$$M_d = \frac{4}{3}\pi R_{dh}^2 R_{d\nu}\rho_d. \tag{4.1}$$

b) The force acted on the drop due to vapor pressure distribution:

Let consider the ellipse determined by following equation:

$$F(x,y) \equiv \frac{x^2}{a^2} + \frac{y^2}{b^2} - 1 = 0, \tag{4.2}$$

where $a = R_{dh}$ and $b = R_{d\nu}$. The normal vector to ellipse is easily calculated:

$$\vec{n} = \frac{\mathrm{grad}F}{|\mathrm{grad}F|} = \frac{1}{\sqrt{\frac{x^2}{a^4} + \frac{y^2}{b^4}}}\left(\frac{x}{a^2}, \frac{y}{b^2}\right) \tag{4.3}$$

and the force acted on the drop is

$$\vec{p} = p_\nu \vec{n} = \frac{p_\nu}{\sqrt{\frac{x^2}{a^4} + \frac{y^2}{b^4}}}\left(\frac{x}{a^2}, \frac{y}{b^2}\right). \tag{4.4}$$

Thus the vertical component of force vector can be calculated

$$p_{||} = \vec{p}\cdot\vec{n} = -\frac{yp_\nu}{b^2\sqrt{\frac{x^2}{a^4} + \frac{y^2}{b^4}}}, \tag{4.5}$$

or in coordinates $x = r\sin\theta$ and $y = r\cos\theta$

$$p_{||} = \vec{p}\cdot\vec{n} = -\frac{p_\nu \cos\theta}{b^2\sqrt{\frac{\sin^2\theta}{a^4} + \frac{\cos^2\theta}{b^4}}}. \tag{4.6}$$

The total force acted on the drop can be calculated by integration along drop surface and has the following form

$$p_{||} = \int_0^{2\pi}\int_0^{\pi} p_{||} r^2 \sin\theta d\theta d\phi = 2\pi \int_0^{\pi} p_{||} r^2 \sin\theta d\theta. \tag{4.7}$$

This integral can be calculated, for example, by trapeze form, cf. Bronstein and Semendjajew 1972 [2].

To determine the initial vapor distribution the system of eqs. (2.5) - (2.9) are used with the following conditions:

$$t = 0 \quad p_\nu(0,\theta) = p_0, \quad \theta = 0 \quad p_\nu(0,\theta) = p_0, \quad \theta = \pi \quad \frac{\partial p_\nu}{\partial \theta} = 0. \tag{4.8}$$

In reality the boundary condition at $\theta = 0$ can be satisfied by releasing small vapour bubble due to difference between vapour and surrounding pressure. During the calculation of steady vapour pressure distribution the drop and bubble positions and shapes are assumed to be fixed.

It should be noted that the vapourisation rate and consequently, the vapour pressure distribution and, therefore, the supported force for drop from surrounding vapour depends on the heat and mass transfer processes between hot drop, vapour and coolant and, consequently, position of drop. The real initial position of drop within the bubble is chosen to be satisfied the force balance condition between the drop weight M_d and support force from surrounding vapour $P_{||}$, i.e.:

$$M_d = p_{||}. \tag{4.9}$$

5. Numerical method

The obtained system of partial differential equations with appropriate initial and boundary conditions at bubble surface, at infinity and along the symmetrical line (2.1)-(2.11) can be solved by combination of the collocation method for definition of outside liquid flow and moving interface with finite difference method for definition of the vapor density and pressure distribution.

The solution of equations (2.1) satisfied the boundary condition (2.3) and without singularity in $\theta = 0$ can be presented in the following form, cf. Abramowitz and Stegun 1970 [1]:

$$\Phi(r,\theta,t) = \sum_{k=0}^{\infty} a_k(t) \frac{1}{r^{k+1}} P_k(\cos\theta). \tag{5.1}$$

In order to apply the collocation method above infinite series is truncated after $N+1$ terms:

$$\Phi(r,\theta,t) = \sum_{k=0}^{N} a_k(t) \frac{1}{r^{k+1}} P_k(\cos\theta), \tag{5.2}$$

here $\{a_k(t)\}_{k=0}^N$ are the coefficients to be chosen to fit the another boundary condition (2.2). Applying collocation on the points $\{\theta_i\}_{i=0}^N$ an appropximate solution with a finite number of expansion coefficients $\{a_k(t)\}_{k=0}^N$ is obtained. From interpolation theory it is known that convergence of series (3.3) for $N \to \infty$ can be guaranteed if $\{\theta_i\}_{i=0}^N$ are the zeros of ultra spherical polynomials, e.g. the Legendre polynomials, cf. Fox and Parker 1968 [4].

The coordinates of the interface $r = R(\theta, t)$ are also expanded in series of Legendre polynomials:

$$R(\theta, t) = \sum_{k=0}^{N} b_k(t) P_k(\cos\theta). \tag{5.3}$$

The numerical procedure to be used is following:

(i) The coefficients $a_k(t)$ (at the beginning $t = 0$) is determined by equations (2.4) and (5.2), the coefficients $b_k(t)$ - by equation (2.11) and (5.3), and the derivatives $\partial\Phi_i/\partial\tau$, $\partial\Phi_i/\partial\theta$, $\partial R_i/\partial\theta$ and $\partial^2 R_i/\partial\theta^2$ can be calculated analytically using (5.2) and (5.3).

(ii) After each time-step Δt the new value of bubble radii R_i will be determined by equation (2.10). Except the first time-step, where the simple Euler integration method has been used, to integrate equation (2.10) the Adams and Bashforth-2 algorithm, cf. Stoer and Bulirsch 1978 [9], is used which takes into account the value of previous gradient:

$$R_i(t + \Delta t) = R_i(t) + 0.5\Big[3\frac{dR_i(t)}{dt} - \frac{dR_i(t - \Delta t)}{dt}\Big]. \tag{5.4}$$

(iii) After each time-step Δt using $R_i(t + \Delta t)$ the new values of vapor density $\rho_{vi}(t + \Delta t)$, vapor pressure $p_i(t + \Delta t)$ and velocity $u_i(t + \Delta t)$ in the gap restricted by drop surface and surrounding liquid will be determined by eqs. (2.5) - (2.9). To solve numerically eq. (2.5) the factorization method [7] is used. It should be noted that eq. (2.5) is non-linear and at each time-step the iteration procedure is used to approach its coefficients.

(iv) The potential $\Phi_i(t + \Delta t)$ is calculated using the last equation in brackets after (2.4) taking into account eq. (2.2). Similar to integration method of eq. (2.10), except the first time-step, where the simple Euler integration method has been used, to integrate this equation the same Adams and Bashforth-2 algorithm is used. After this the procedure is repeated for each time-step consecutively.

Finite difference scheme and iteration procedure: To solve numerically eq. (2.5) with initial and boundary conditions (2.8), (2.9) the following finite difference scheme is used:

$$\frac{1}{\Delta t}\left[\left(\frac{R_b^3-R_d^3}{3}\rho_\nu\right)_i^{n+1,k+1}-\left(\frac{R_b^3-R_d^3}{3}\rho_\nu\right)_i^{n}\right]=\left(D^2+jR_b^2\right)_i^{n+1,k+1}, \qquad (5.5)$$

where

$$\left(D^2\right)_i^{n+1,k+1}=\frac{n}{k\mu_\nu\sin\beta_i}\frac{1}{0.5(\beta_{i+1}-\beta_{i-1})}\times$$

$$\times\left\{\mathbb{C}_{i+0.5}^{n+1,k}\frac{\left(\rho_{\nu i+1}-\rho_{\nu i}\right)^{n+1,k+1}}{\beta_{i+1}-\beta_i}-\mathbb{C}_{i-0.5}^{n+1,k}\frac{\left(\rho_{\nu i}-\rho_{\nu i-1}\right)^{n+1,k+1}}{\beta_i-\beta_{i-1}}\right\},$$

$$\mathbb{C}=(R_b-R_d)^3p_\nu\sin\beta,\quad \beta=\pi-\theta,\quad (\beta_0=0,\ \beta_N=2\pi),\quad i=1,2,\ldots,N-1.$$

The equation (5.5) can be rewritten in the following form suitable for numerical integration using the method of factorization:

$$-A_i\rho_{\nu i+1}^{n+1,k+1}+B_i\rho_{\nu i}^{n+1,k+1}-C_i\rho_{\nu i-1}^{n+1,k+1}=D_i, \qquad (5.6)$$

where

$$A_i=\Delta tK_i^{n+1}p_{i+0.5}^{n+1,k};$$

$$B_i=1+\Delta tK_i^{n+1}\left(p_{i+0.5}^{n+1,k}+p_{i-0.5}^{n+1,k}\right);$$

$$C_i=\Delta tK_i^{n+1}p_{i-0.5}^{n+1,k};$$

$$D_i=\frac{\left(R_b^3-R_d^3\right)_i^n}{\left(R_b^3-R_d^3\right)_i^{n+1}}+3\Delta t\left(\frac{j^kR_b^2}{R_b^3-R_d^3}\right)_i^{n+1};$$

$$K_i^{n+1}=\frac{3n}{k\mu_\nu\sin\beta_i\left(R_b^3-R_d^3\right)_i^{n+1}};$$

$$P_{i+0.5}^{n+1,k}=\frac{2\left[(R_b-R_d)^3p_\nu\sin\beta\right]_{i+0.5}^{n+1,k}}{(\beta_{i+1}-\beta_{i-1})(\beta_{i+1}-\beta_i)};$$

$$P_{i-0,5}^{n+1,k}=\frac{2\left[(R_b-R_d)^3p_\nu\sin\beta\right]_{i-0.5}^{n+1,k}}{(\beta_{i+1}-\beta_{i-1})(\beta_i-\beta_{i-1})};$$

$$i=1,2,\ldots,N-1.$$

And in according to used calculation method we have:

$$\rho_{\nu i}^{n+1,k+1}=\gamma_i\rho_{\nu i+1}^{n+1,k+1}+\eta_i, \qquad (5.7)$$

where

$$\gamma_i = \frac{A_i}{B_i - C_i\gamma_{i-1}}, \quad \eta_i = \frac{D_i + C_i\eta_{i-1}}{B_i - C_i\gamma_{i-1}}, \quad i = 1, 2, \ldots, N-1.$$

Additionally in according to boundary conditions, we have, respectively:

$$\begin{aligned} \rho_{\nu N}^{n+1,k+1} &= \rho_{\nu N-1}^{n+1,k+1}, \quad \text{(at point } i = N\text{)}, \\ \rho_{\nu 0}^{n+1,k+1} &= \rho_{\nu 1}^{n+1,k+1}, \quad \text{(at point } i = 0\text{)}. \end{aligned} \tag{5.8}$$

Thus from equations (5.7) and (5.8) we have:

$$\begin{aligned} &\rho_{\nu N-1} = \frac{\eta_{N-1}}{1 - \gamma_{N-1}}, \quad \text{(at point } i = N-1\text{)}, \\ &\gamma_0 = 1, \quad \eta_0 = 0, \quad \text{(at point } i = 0\text{)}, \end{aligned} \tag{5.9}$$

For initial installation in according to two last conditions of (4.8) instead of (5.9) we have:

$$\begin{aligned} &\rho_{\nu N} = \rho_{\nu N}(t = 0) = \text{const}, \quad \text{(at point } i = N\text{)}, \\ &\gamma_0 = 1, \quad \eta_0 = 0, \quad \text{(at point } i = 0\text{)}. \end{aligned} \tag{5.10}$$

The considered above finite difference scheme is implicit. It is easily to show that it is stable, i.e. the approach errors at least are not increased from step to step, because the coefficients A_i, B_i, C_i satisfy following conditions

$$\begin{aligned} &A_i, \quad B_i, \quad C_i > 0, \\ &B_i = 1 + A_i + C_i > A_i + C_i > 0. \end{aligned} \tag{5.11}$$

Using Taylor expansion (e.g. Wachspress 1966 [12]) or method of box integration (e.g. Runchal, Spalding and Wolfschtein 1969 [8]) it can be shown that for nonuniform grids the presented above finite difference scheme has the first-order accuracy, i.e. a precision of order $O(\Delta t, \Delta\theta)$, and for uniform grids - a precision of order $O(\Delta t, (\Delta\theta)^2)$. The nonuniform mesh cell structure taken into account specific characteristics of considered problem is also used by Thoman and Szewczyk 1969 [10].

Let us consider the following example nonlinear differential equation:

$$\frac{\partial \rho}{\partial t} + f(\beta)\frac{\partial}{\partial \beta}\left(g(\rho, \beta)\frac{\partial \rho}{\partial \beta}\right) = 0. \tag{5.12}$$

Let consider the Taylor expansion at point i:

$$\rho_i^{n+1} = \rho_i^n + \Delta t\Big(\frac{\partial \rho}{\partial t}\Big)_i^n + 0((\Delta t)^2), \tag{5.13}$$

$$\rho_{i+1} = \rho_{i+0.5} + 0.5(\beta_{i+1} - \beta_i)\Big(\frac{\partial \rho}{\partial \beta}\Big)_{i+0.5} + 0.5\big(0.5(\beta_{i+1} - \beta_i)\big)^2\Big(\frac{\partial^2 \rho}{\partial \beta^2}\Big)_{i+0.5} + 0((\Delta\beta)^3);$$

$$\rho_i = \rho_{i+0.5} - 0.5(\beta_{i+1} - \beta_i)\Big(\frac{\partial \rho}{\partial \beta}\Big)_{i+0.5} + 0.5\big(0.5(\beta_{i+1} - \beta_i)\big)^2\Big(\frac{\partial^2 \rho}{\partial \beta^2}\Big)_{i+0.5} + 0((\Delta\beta)^3);$$

$$g_{i+0.5}\Big(\frac{\partial \rho}{\partial \beta}\Big)_{i+0.5} = g_i\Big(\frac{\partial \rho}{\partial \beta}\Big)_i + 0.5(\beta_{i+1} - \beta_i)\frac{\partial}{\partial \beta}\Big(g\frac{\partial \rho}{\partial \beta}\Big)_i + 0((\Delta\beta)^2),$$

$$g_{i-0.5}\Big(\frac{\partial \rho}{\partial \beta}\Big)_{i-0.5} = g_i\Big(\frac{\partial \rho}{\partial \beta}\Big)_i - 0.5(\beta_i - \beta_{i-1})\frac{\partial}{\partial \beta}\Big(g\frac{\partial \rho}{\partial \beta}\Big)_i + 0((\Delta\beta)^2).$$

Therefore we have:

$$\Big(\frac{\partial \rho}{\partial t}\Big)_i = \frac{\rho_i^{n+1} - \rho_i^n}{\Delta t} + 0(\Delta t),$$

$$\Big(\frac{\partial \rho}{\partial \beta}\Big)_{i+0.5} = \frac{\rho_{i+1} - \rho_i}{\beta_{i+1} - \beta_i} + 0((\Delta\beta)^2), \tag{5.14}$$

$$\Big(\frac{\partial \rho}{\partial \beta}\Big)_{i-0.5} = \frac{\rho_i - \rho_{i-1}}{\beta_i - \beta_{i-1}} + 0((\Delta\beta)^2),$$

$$\frac{\partial}{\partial \beta}\Big(g\frac{\partial \rho}{\partial \beta}\Big)_i = \frac{\Big[g\Big(\frac{\partial \rho}{\partial \beta}\Big)\Big]_{i+0.5} - \Big[g\Big(\frac{\partial \rho}{\partial \beta}\Big)\Big]_{i-0.5}}{0.5(\beta_{i+1} - \beta_{i-1})} + 0(\Delta\beta).$$

Using the uniform mesh cell structure the finite difference scheme precision can be improved to space second-order accuracy.

For iteration all parameters at $k = 0$ take initial value from previous time step, i.e. $\rho_{\nu i}^{n+1,0} = \rho_i^n$, $\rho_{\nu i}^{n+1,0} = \rho_{\nu i}^n$ and so on. It should be noted that the value of bubble radius R_{bi}^{n+1} should not be iterated, because in every timestep it already determined before calculating vapour characteristics. The iteration will be interrupted in according to following criteria:

$$\frac{\rho_{\nu i}^{n+1,k+1} - \rho_{\nu i}^{n+1,k}}{\rho_{\nu i}^{n+1,k+1}} < \varepsilon, \quad \varepsilon = 10^{-7}, \quad i = 0, 1, 2, \ldots, N. \tag{5.15}$$

6. Calculation results

In Figs. 2-4 the calculation results are presented for cases of spherical steam bubble with radius $R_{b0} = 5\,\text{mm}$ and alumina drop with radius $R_d = 2.5\,\text{mm}$ in water without ($j = 0$) (Fig. 2, 3) and with heat-mass transfer ($j \neq 0$) (Fig. 4). In these cases the centers of bubbles and drops, proposed, coincide. In accordance to Grigul, 1989 [5] and Vargaftik, 1975 [11] the thermo- and physical properties of fluid and vapor are following: $T_0 = 373\,\text{K}$; $T_d = 1570\,\text{K}$; $T_v = 970\,\text{K}$; $c_v = 2270$ J/kgK; $\lambda_v = 0.1\,\text{W/mK}$; $n = 1.26$; $\rho_{v0} = 0.22\,\text{kg/m}^3$; $\mu_v = 4 \times 10^{-5}\,\text{Ns/m}^2$; $\sigma = 5.3 \times 10^{-2}\,\text{kg/s}$; $l = 2100\,\text{kJ/kg}$; $g = 9.8\,\text{m/s}^2$; $\rho_\ell = 998\,\text{kg/m}^3$; $\rho_d = 3500\,\text{kg/m}^3$; $\varepsilon = 3.5$; $B = 5.67 \times 10^{-8}\,\text{W/m}^2\text{K}^4$.

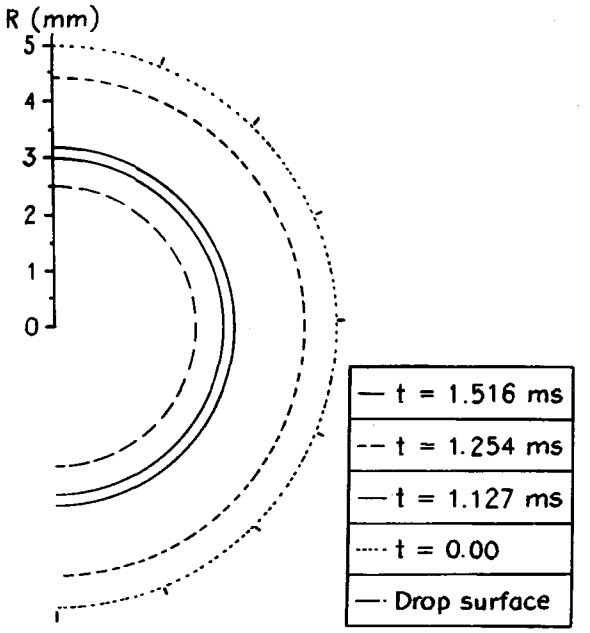

Fig. 2

In Fig. 3 the numerical results at $t \to +\infty$ are compared with limited values, which in this case can be obtained by analytical methods. There are good agreements between the numerical and analytical solutions. In the case with mass transfer the vapor density approachs the limited value, and the radius increases (Fig. 4).

In Fig. 5 the scheme of experiment is presented. The pressure pulses are created by magnetic hammer (Peppler, Till and Kaiser 1991 [6]). In Figs. 6-8 presented the numerical and experimental results for following case: $R_{bv} = 3.7\,\text{mm}$; $R_{bh} = 3.6\,\text{mm}$; $R_{dv} = R_{dh} = 2.7\,\text{mm}$; $T_0 = 373\,\text{K}$; $T_d = 2569\,\text{K}$; $T_v = 1430\,\text{K}$;

$c_v = 2622\,\mathrm{J/kgK}$; $\lambda_v = 0.195\,\mathrm{W/mK}$; $n = 1.22$; $\rho_{v0} = 0.150\,\mathrm{kg/m^3}$; $\mu_v = 2.1 \times 10^{-5}\,\mathrm{Ns/m^2}$; $\sigma = 5.3 \times 10^{-2}\,\mathrm{kg/s}$; $l = 2100\,\mathrm{kJ/kg}$; $g = 9.8\,\mathrm{m/s^2}$; $\rho_\ell = 998\,\mathrm{kg/m^3}$; $\rho_d = 3500\,\mathrm{kg/m^3}$; $\varepsilon = 3.5$; $B = 5.67 \times 10^{-8}\,\mathrm{W/m^2K^4}$.

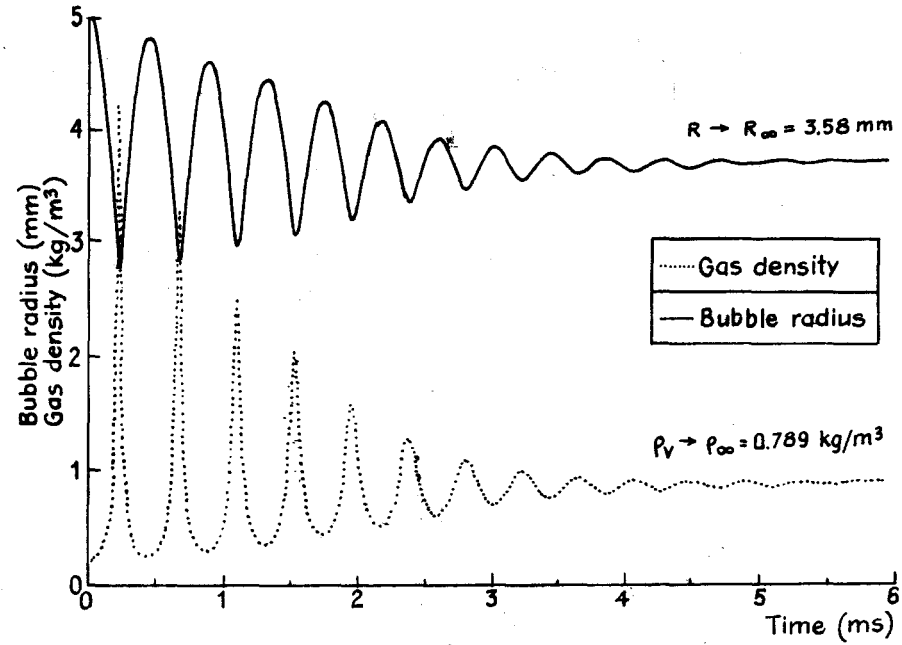

Fig. 3

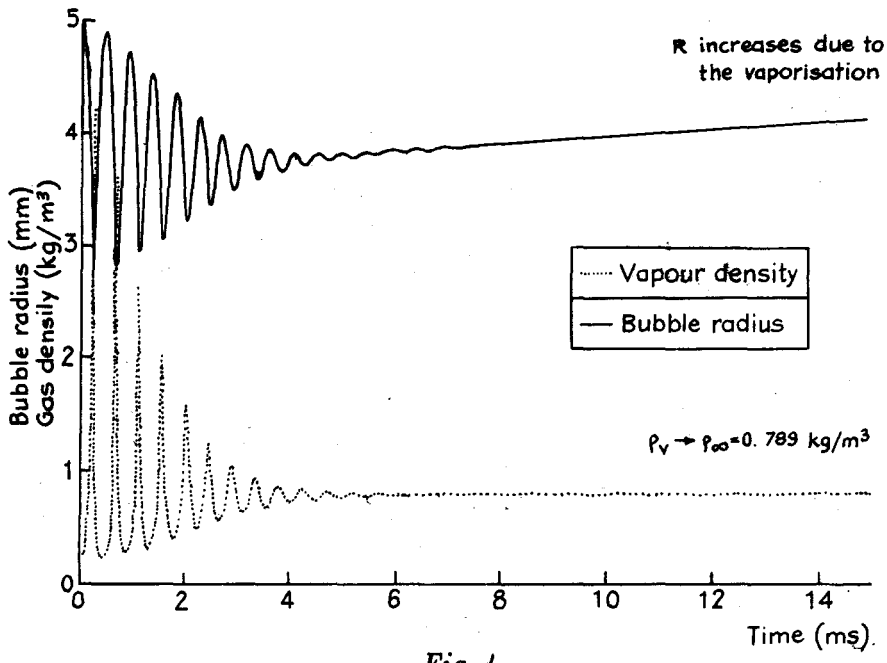

Fig. 4

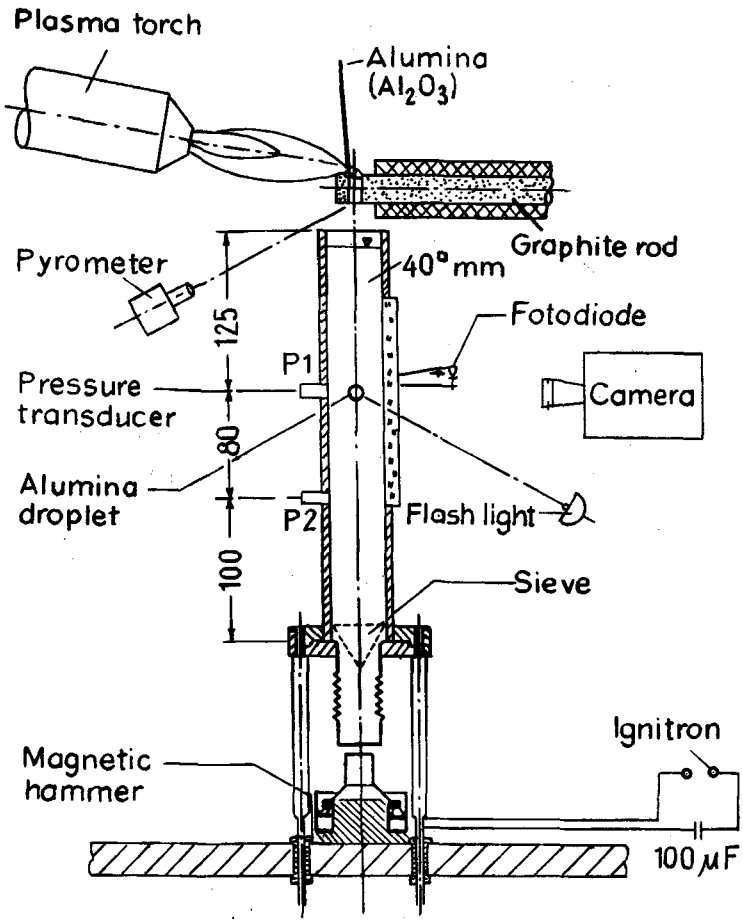

Fig. 5

From Fig. 6 it can be seen that the calculation results described quantitatively good two phases of considered process: the first compress phase and the second expansion phase. In Fig. 7 pressure distribution in some moments are presented. In Fig. 8 comparison of calculation results (bubble diameter equator) and experiment is presented. It should be noted that at the beginning part of the second phase, i.e. at the time between 0.2 and 0.5 ms, in experiment the expansion is occurred mainly at the top part of drop, meanwhile in calculation this process is occurred in all directions. In compress phase the bubble surface stays smooth. In expansion phase wave is observed in both experiment and calculation. The vapor velocity and vapor parameters (pressure and density) quickly have a uniform distribution. At moment $t = 0.53$ ms vapor mostly does not move along the gap.

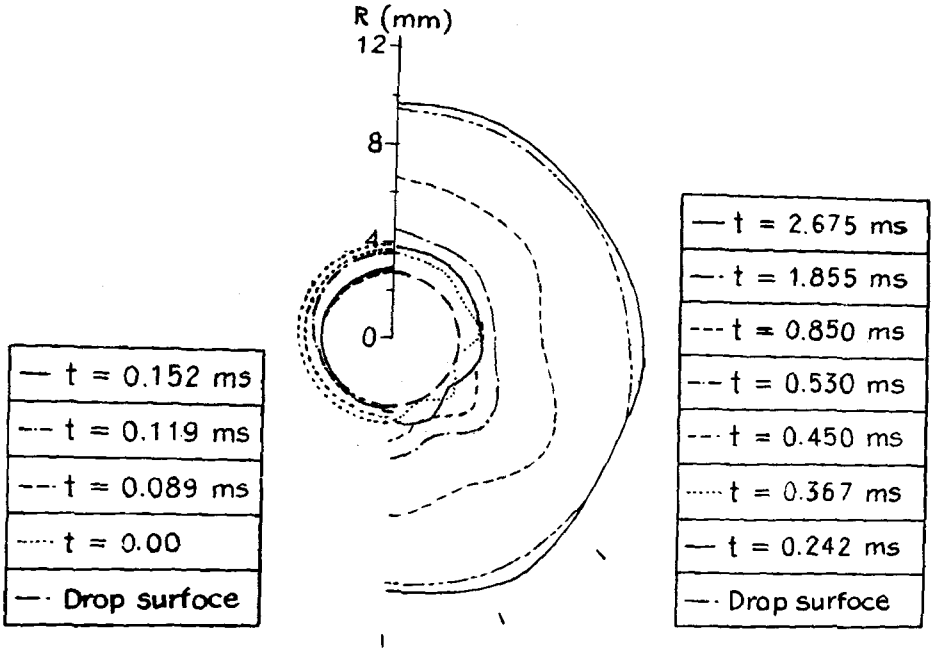
R (mm)
12
8
4
0
— t = 0.152 ms
--- t = 0.119 ms
---- t = 0.089 ms
..... t = 0.00
—· Drop surfoce
— t = 2.675 ms
—· t = 1.855 ms
--- t = 0.850 ms
—·· t = 0.530 ms
---· t = 0.450 ms
..... t = 0.367 ms
— t = 0.242 ms
—· Drop surfoce

Fig. 6

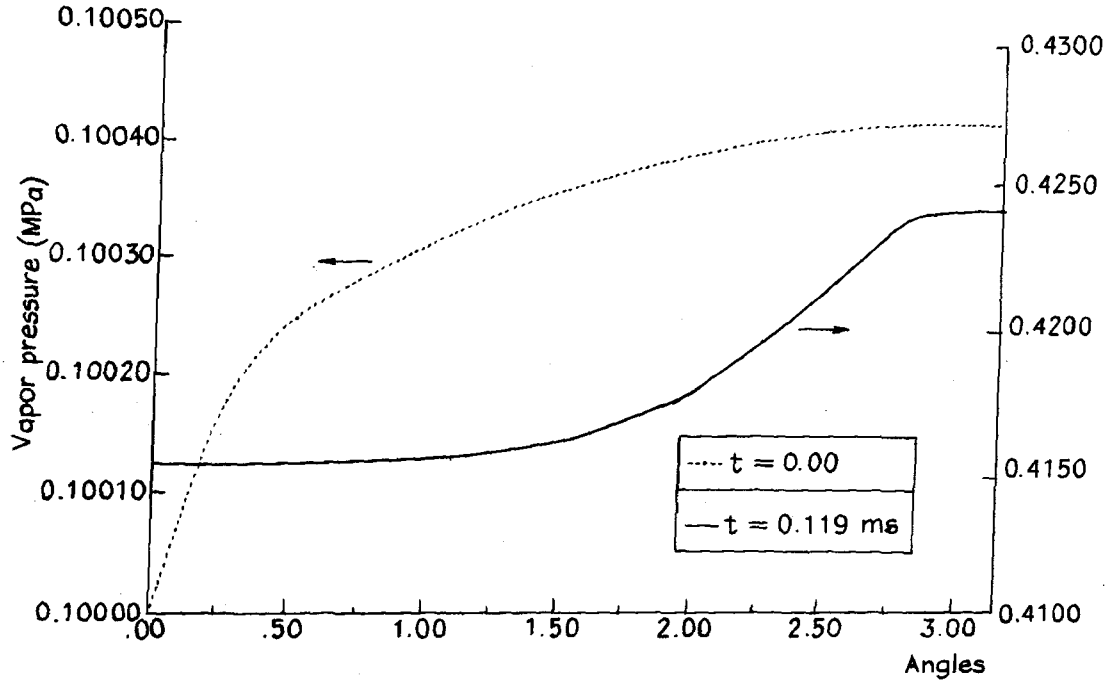
0.10050
0.10040
0.10030
0.10020
0.10010
0.10000
Vapor pressure (MPa)
0.4300
0.4250
0.4200
0.4150
0.4100
.00
.50
1.00
1.50
2.00
2.50
3.00
Angles
..... t = 0.00
— t = 0.119 ms

Fig. 7

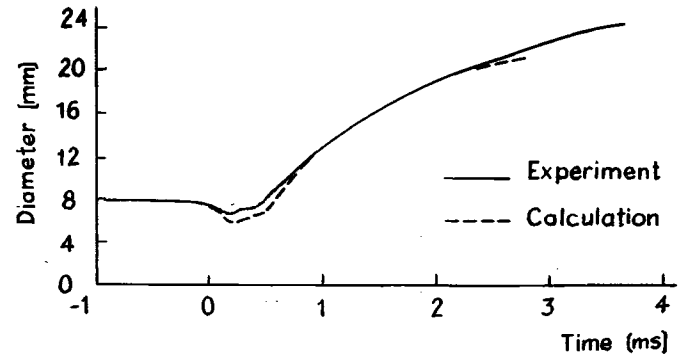

Fig. 8

7. Conclusion

For bubble - inside drop system within the framework of mathematical model taking into account the thermal conditions, heat and mass transfer between phases, the collapse process caused by pressure increasing in surrounding fluid in film boiling condition is investigated. The problem is multi-parametric. In total, 17 dimensionless parameters and combinations characterize solution set. The obtained results show the important role of geometrical, thermal conditions, thermo-physic properties of phases and heat-mass transfer process. The calculation results are quantitatively good agreed with experimental observation.

Acknowledgements. The research is completed with financial support of The Alexander von Humboldt Foundation (Germany) and Vietnam National Basic Research Foundation in Natural Sciences, to which the author would like to express his sincere thanks.

Nomenclature

a_0 sound velocity in gas [m/s^2],
a_k expansion coefficient, function of k and t,
b_k expansion coefficient, function of k and t,
B coefficient Stefan-Boltzmann [W/m^{2}K^4],
c specific heat capacity at constant pressure [j/kgK],
$D = \lambda/\rho c$, thermal diffusivity [m^2/s],
g gravitational acceleration [m/s^2],
j rate of phase transition per unit interfacial surface [kg/m^{2}s],
k coefficient in formula (7),

l latent of evapourisation [j/kg],
n polytropic coefficient,
N maximum number of collocation angles,
p pressure [Pa].
P_k k-th Legendre polynomial,
q heat flux [j/m^{2}s],
r radial co-ordinate in spherical co-ordinates [m],
R drop and bubble radius in spherical co-ordinates [m],
t time [s],
T absolute temperature [K],
u velocity [m/s],
x bubble surface coordinate or horizontal coordinate [m],
y vertial coordinate [m].

Greek symbols

$\beta = \pi - \theta$,
δ thermal boundary-layer thickness in liquid [m],
Δt timestep,
$\Delta\theta$ angle-step,
ε emission coefficient or precision,
θ azimuthal angle in spherical co-ordinates,
λ thermal conductivity [W/mK],
μ vapour dynamic viscosity [Ns/m^2],
ρ density [kg/m^3],
σ surface tension coefficient [N/m],
Φ velocity potential in vortex-free flow [m^2/s].

Subscripts

b bubble,
c convective,
d drop,
eq equivalent,
g gas,
h horizotal,
i number of a collocation point,
l liquid,
O characterized value or parameter of initial state,
r radiation or radial direction,
s saturated,
v vapour (for p, ρ and u) or vertical for R),

θ tangential direction,
∞ at infinity.

Superscripts

k iteration number,
n number of timestep.

REFERENCES

1. Abramowitz M. and Stegun I. A. Handbook of Mathematical Functions with Formulas, Graphs and Mathematical Tables. Dover Publ. Inc., New York, 1970.

2. Bronstein I. N. and Semendjajew K. A. Taschenbuch der Mathematik. Verlag Harri Deutsch, Franfurt/Main, 1972.

3. Duong Ngoc Hai. Obtaining Equation Set for Two - Phase Bubble Dynamic Description. J. Mechanics, Vol.17, No.2, 1995.

4. Fox L. and Parker I. B. Cherbyshev Polynomials in Numerical Analysis. Oxford Univ. Press, London, 1968.

5. Grigul U. (Ed.) Properties of Water and Steam in SI-Units. Springer Verl., Berlin, 1989.

6. Peppler W., Till W. and Kaiser A. Experiments on Thermal Interactions: Test with Al_2O_3 Droplets and Water. KfK 4891, Karlsruhe, 1991.

7. Richtmyer R. D. and Morton K. W. Difference Methods for Initial - Value Problems. Interscience Publ., Division of John Wiley and Sons, 1967.

8. Runchal A. K., Spalding D. B. and Wolfshtein M. Numerical Solution the Elliptic Equations for Transport of Vorticity, Heat and Matter in Two-Dimensional Flow. In: High - Speed Computing in Fluid Dynamics/ The Physics of Fluid Supplement II. (Eds. Freukiel F. N. and Stewartson K.), American Inst. of Physics, New York, 1969.

9. Stoer J. and Bulirsch R. Einfuhrung in die Numerische Mathematik. Springer Verl., New York, 1978.

10. Thoman D. C. and Szewczyk A. A. Time-Dependent Viscous Flow over a Circular Cylinder. In: High - Speed Computing in Fluid Dynamics/ The Physics of Fluid Supplement II. (Eds. Freukiel F. N. and Stewartson K.), American Inst. of Physics, New York, 1969.

11. Vargaftik N. B. Tables on the Thermophysical Properties of Liquids and Gases. Hemisphere Publ. Co., Washington, 1975.

12. Wachspress E. L. Iterative Solution of Elliptic Systems (and Application to the Neutron Diffusion Equations of Reactor Physics). Prentice-Hall Inc., Englewood Cliffs, New Jersey, 1966.

Received March 15, 1999

ỨNG DỤNG KẾT HỢP PHƯƠNG PHÁP ĐỊNH VỊ
VÀ PHƯƠNG PHÁP NHÂN TỬ HÓA
ĐỂ GIẢI BÀI TOÁN ĐỘNG LỰC HỆ BỌT-HẠT Ở TRONG

Bài báo trình bày việc sử dụng kết hợp phương pháp định vị và phương pháp nhân tử hóa để giải bài toán động lực hệ bọt-hạt ở trong. Ở trạng thái ban đầu bọt và hạt giả thiết có dạng elippsoid. Vị trí tương đối ban đầu của hạt trong bọt được xác định từ điều kiện cân bằng giữa trọng lượng của hạt và lực nâng do phân bố áp suất trong khí / hơi. Tính toán được thực hiện cho trường hợp bọt, hạt cầu khi không có và khi có bay hơi (hiệu ứng nhiệt) và cho trường hợp thí nghiệm [6] hạt nhôm lỏng trong nước khi có sóng áp suất.

Institute of Mechanics, NCST of Vietnam
264 Doi-Can-Str., Hanoi, Vietnam
Tel. 84.4.8329706, Fax: 84.4.8333039
E-mail: dnhai @ im 01.ac.vn